LWT - Food Science and Technology 172 (2022) 114200

Contents lists available at ScienceDirect

LWT

journal homepage: www.elsevier.com/locate/lwt

Ethylene scavenging film based on low-density polyethylene incorporating pumice and potassium permanganate and its application to preserve avocados

Chunyu Wang, Abdellah Ajji *

3SPack, Research Center for High Performance Polymer and Composite Systems CREPEC, Chemical Engineering Department, Polytechnique Montréal, Montréal, Québec, H3C 3A7, Canada

ARTICLE INFO

Keywords:
Pumice
$KMnO_4$
Avocados
Ethylene scavenging
CO_2 concentration

ABSTRACT

The ethylene scavenging film was prepared to extend the shelf life of fresh fruit and vegetables. This film consisted of low-density polyethylene (LDPE) as matrix, the mixture of pumice and potassium permanganate ($KMnO_4$) (weight ratio: 10 to 1) (pumice acted as the support of $KMnO_4$) as active agents, and maleic anhydride grafted polyethylene (PE-g-MA) as compatibilizer. The study revealed that low loadings of active agents (1 wt% and 3 wt%) were evenly distributed in the LDPE matrix and were beneficial to the improvement of the mechanical property, crystallinity, and gas barrier performance against oxygen and water vapor. In addition, the film (thickness: 60 μm) incorporating 3 wt% active agents had an ethylene scavenging capacity of 7.31 μmol/(25 in^2) within 12 d at 25 °C. Further, the ethylene scavenging film with 3 wt% active agents preserved avocados well for 20 d at 25 °C, inhibited the ethylene and carbon dioxide (CO_2) concentrations in the packaging headspace, and reduced the flesh firmness loss, while the shelf life of avocados packaged with pure LDPE film was only 10 d.

1. Introduction

The loss of fruit and vegetables is a troublesome problem around the world because a large proportion (nearly 50% of food loss) of postharvest products turn rotten during transportation, storage, and sale (Blanke, 2014). In the process of maturation, fruit and vegetables release ethylene that in turn accelerates their ripening and senescence (Gaikwad et al., 2019; Pathak et al., 2017; Wei et al., 2021). Hence, the shelf life of fruit and vegetables would be extended if ethylene produced in the packaging headspace is scavenged (Sultana et al., 2022; Álvarez-Hernández et al., 2018, 2019a). Active packaging technology is a suitable method to scavenge ethylene to preserve fruit and vegetables (Boonsiriwit et al., 2020; Keller et al., 2013; Wyrwa & Barska, 2017), and active packaging films are equipped with ethylene scavenging ability owing to the incorporation of active agents.

Potassium permanganate ($KMnO_4$) is an effective active agent that oxidizes ethylene into water and carbon dioxide (CO_2), and the stoichiometric oxidation reaction is: $3C_2H_4 + 12KMnO_4 \rightarrow 12MnO_2 + 12KOH + 6CO_2$ (Wei et al., 2021; Zhang et al., 2017). Although $KMnO_4$ is a chemical substance and the toxicity is a concern to people, it has been regarded as an eco-friendly oxidising agent and widely used in environmental protection to neutralise some contaminants, such as trichloroethylene, pesticides, and alkaloid toxins (Dash et al., 2009; Singh & Lee, 2001). It may be lethal when the $KMnO_4$ dose reaches 142.9 mg/kg per person (Álvarez-Hernández et al., 2018), which means that 10 g of $KMnO_4$ may cause intoxication for a person who weighs 70 kg (Cevik et al., 2012). Actually, it is difficult for an adult to ingest so much $KMnO_4$. This is because on the one hand, the content of $KMnO_4$ used in active packaging materials is generally low (Ebrahimi et al., 2021; Joung et al., 2021; Álvarez-Hernández et al., 2018). On the other, if a small amount of $KMnO_4$ migrates to the surface of fruit and vegetables, it is easily washed off by water as 100 mL of water can dissolve 6.4 g and 25 g of $KMnO_4$ at 20 °C and 65 °C respectively (NCBI, 2022).

A few years ago, one active packaging film was developed by embedding $KMnO_4$ into LDPE, which not only had improved oxygen barrier performance but also prolonged the shelf life of bananas up to twice based on the peel color index (Khosravi et al., 2013). However, it is rare to apply $KMnO_4$ as active agent alone because its ethylene-oxidizing efficiency is related to the surface area of $KMnO_4$ exposed to ethylene (Wang, Chunyu and Ajji, Abdellah, 2022; Wills & Warton, 2004).

* Corresponding author.
E-mail addresses: chunyu.wang@polymtl.ca (C. Wang), abdellah.ajji@polymtl.ca (A. Ajji).

https://doi.org/10.1016/j.lwt.2022.114200
Received 26 July 2022; Received in revised form 20 October 2022; Accepted 20 November 2022
Available online 27 November 2022

Therefore, $KMnO_4$ is generally combined with support materials with high specific surface area (Widayanti et al., 2016; Álvarez-Hernández et al., 2019b, 2020). Recently, an ethylene scavenging film containing $KMnO_4$-impregnated halloysite was prepared to extend the shelf life of cherry tomatoes by lowering the ethylene and CO_2 production rate (Joung et al., 2021). However, two weaknesses may exist in that research: $KMnO_4$ used in the initial stage could not adhere completely to halloysite by means of solution soaking-vacuum-drying method, and no compatibilizer was used to improve the compatibility between halloysite and low-density polyethylene (LDPE).

LDPE, one of the most common polymers, is used as packaging films owing to good flexibility, durability, mechanical and water barrier properties, as well as some advantages including nontoxicity, low cost, and abundant resources (Kordjazi & Ajji, 2021; Monprasit et al., 2011; Reesha et al., 2015). Pumice is a porous volcanic rock formed during volcanic eruptions, and it possesses some advantages, including low cost, high porosity, good adsorption property, easy availability, and eco-friendly nature (Heibati et al., 2014; Ismail et al., 2014; Rad et al., 2018). In the system of pumice and $KMnO_4$, pumice can physically adsorb ethylene and act as the support to increase the specific surface area of $KMnO_4$ exposed to ethylene (Wang, Chunyu and Ajji, Abdellah, 2022).

In this study, the two weaknesses mentioned earlier were tackled by direct grinding combination of pumice and $KMnO_4$ and the application of compatibilizer. The mixture of pumice and $KMnO_4$ was employed as active agents, LDPE as matrix, and maleic anhydride grafted polyethylene (PE-g-MA) as compatibilizer to prepare ethylene scavenging films. First, the films with different content of active agents were prepared via a twin-screw extruder. Then, the dispersion of active agents, thermal and mechanical performance, ethylene scavenging capacity, and gas barrier properties of prepared films were characterized and compared. Next, the films were applied to preserve avocados, and gas composition in packaging headspace and the flesh firmness were further analyzed. Finally, the safety evaluation was carried out by investigating the migration of active agents. To the best of our knowledge, the preparation of ethylene scavenging films by incorporating pumice and $KMnO_4$ into LDPE films has not been studied yet.

2. Experimental

2.1. Materials

Pumice (size: 2 μm–45 μm) was supplied by Hess Pumice Company, Idaho, USA. $KMnO_4$ was purchased from Thermo Fisher Scientific, Canada. Ethylene was from Air Liquide, Canada. LDPE (NOVAPOL® LF-0219-A, density (23 °C): 0.918 g/cm^3, melt index (190 °C/2.16 kg): 2.3 g/10 min) was acquired from Nova Chemical Corporation, Alberta, Canada. PE-g-MA (BYNEL™ 4206, density (23 °C): 0.92 g/cm^3, melt index (190 °C/2.16 kg): 2.5 g/10 min) was acquired from Dow Chemical Company, Ontario, Canada. Avocados (Delicia avocado, Mexico) were air-transferred to Canada once picked from trees in Mexico, and no more treatment was performed before experiment. Avocados without visual defects were collected from Walmart supermarket and selected to ensure uniformity in terms of shape and weight (180 ± 10 g). When choosing avocados, one should make sure that they had the following features, hard texture when squeezing, tough mouthfeel, green flesh, and unripe odor (Kokawa et al., 2020).

2.2. Sample preparation

Pumice was sieved with mesh sieve (opening: 2500, pore size: 5 μm) to obtain particles size in the range of 2–5 μm, and the specific surface area and pore volume were 11.701 m^2/g and 0.045 cc/g respectively. Then, pumice and $KMnO_4$, with a weight ratio of 10 to 1, were mixed and ground for at least 30 min through grinding ball mill (SPEX Sample Prep 8000 Series Mixer), until achieving uniformity. Herein, pumice served as the support of $KMnO_4$ and the weight ratio of 10:1 (pumice to $KMnO_4$) was obtained according to our previous research (Wang, Chunyu and Ajji, Abdellah, 2022), which revealed that the combination of pumice and $KMnO_4$ was able to remove much more ethylene than pumice or $KMnO_4$ alone due to the synergistic effect of pumice adsorbing ethylene and $KMnO_4$ oxidizing ethylene. Hence, the films incorporating $KMnO_4$ or pumice alone were not investigated in depth in this study. LDPE and PE-g-MA were dried at 70 °C overnight in a vacuum oven before melt blending. Subsequently, LDPE, PE-g-MA, and the mixture of pumice and $KMnO_4$ were extruded by the twin-screw extruder (Leistritz Extrusionstechnik GmbH, ZSE18HP-40D, screw diameter: 18 mm) and made into films via a casting die at a screw speed of 50 rpm and a temperature profile of 150–170 °C. Herein, the amount of mixture (pumice and $KMnO_4$) was 1 wt%, 3 wt%, 5 wt%, and 10 wt% respectively. The corresponding PE-g-MA content was also added at 1 wt %, 3 wt%, 5 wt%, and 10 wt% respectively. Finally, the thickness of the films was controlled at approximately 60 μm. For the sake of convenient presentation, these LDPE-based films were denoted as LDPE-1%PKM, LDPE-3%PKM, LDPE-5%PKM, and LDPE-10%PKM, respectively, where PKM means the mixture of pumice and $KMnO_4$, and pure LDPE film was prepared as control.

2.3. Characterization of LDPE-based films

2.3.1. Scanning electron microscopy (SEM) and surface color

SEM (Hitachi TM3030Plus equipment) was used to observe the cross-section of cryo-fractured films at a voltage of 15 kV. Samples were treated with liquid nitrogen for 15 min and then snapped before being observed by SEM.

The surface color of films was measured using CR20 Colorimeter (Hangzhou CHNSpec Technology co. ltd, China) with a measuring aperture of 4 mm in diameter. The parameters of L*, a*, and b* represent lightness, redness/greenness, and yellowness/blueness respectively. Herein, the color of pure LDPE film placed upon the white plate was chosen as the reference used to compare the color change of films. The color difference (ΔE*) was calculated according to the equation:

$$\Delta E^* = \sqrt{\Delta L^{*2} + \Delta a^{*2} + \Delta b^{*2}}$$

Where ΔL* = L* reference – L* test sample, Δa* = a* reference – a* test sample, Δb* = b* reference – b* test sample.

2.3.2. Fourier transform infrared spectroscopy (FTIR)

FTIR spectrophotometer (PerkinElmer) was used to monitor the difference between films, PE-g-MA, and active agents. Samples were scanned from 4000 to 600 cm^{-1} at a scanning resolution of 4 cm^{-1} and the spectra between 630 and 3300 cm^{-1} were analyzed.

2.3.3. Differential scanning calorimetry (DSC)

DSC (Q1000, TA Instrument) was conducted to analyze the thermal behavior of films under nitrogen atmosphere. At first, samples were heated from 40 °C to 160 °C to eliminate thermal history at a heating rate of 10 °C/min. After isothermal equilibrium for 5 min, samples were cooled to 40 °C at a cooling rate of 10 °C/min and finally were heated again to 160 °C at a heating rate of 10 °C/min.

2.3.4. Mechanical properties

The mechanical properties of the films were obtained by a universal testing machine (Bluehill Instron) with a sample strip width of 0.5 cm, a load cell 50 kgf, a gauge length of 50 mm, and a crosshead speed of 500 mm/min. Each film was tested ten times and all data including Young's modulus, tensile strength, and elongation at break were reported.

2.3.5. Gas barrier properties

The oxygen transmission rate (OTR) of films was measured using MOCON OX-TRAN Model 2/21 (Minneapolis, USA) at 23 °C, 0% relative humidity, and 1 atm pressure. The water vapor transmission rate (WVTR) was tested via MOCON AQUATRAN Model 1 (Minneapolis, USA) at 38 °C, 90% relative humidity, and 1 atm pressure. The units of OTR and WVTR were cc/[m^2·day] and g/[m^2·day] respectively.

2.3.6. Ethylene scavenging capacity

All films with the same thickness of nearly 60 μm were cut to a size of 5 × 5 in^2. Subsequently, these films were placed in sealed containers with the volume of 1 L at 25 °C and 30% relative humidity, followed by the injection of 200 μL of ethylene with a syringe. Ethylene content was measured each day using F-950 Three Gas Analyzer (Felix Instruments, USA) with gas inlet and outlet connecting sampling probes. During detection, the gas in the headspace is pumped into the analyzer at a sampling flow rate of 70 mL/min and a sampling volume of 35 mL. After detection, the gas is pumped back to the headspace to prevent vacuum from occurring. Finally, ethylene scavenging capacity of films was obtained by calculating the difference between the initial amount of ethylene and the remaining amount in containers, and the unit was expressed as μmol/(25 in^2).

2.4. Packaging avocados

The films were applied to preserve avocados at 25 °C and 30% of relative humidity. Firstly, cut films to the same size of 20 × 8 in^2, and then packaged avocados with the aid of 20'' Impulse Sealer (Model NO. H-1029). Each film was prepared as two replicates assigned #1 and #2. Ethylene, CO_2, and oxygen (O_2) concentrations in packaging headspace were measured every two days using F-950 Three Gas Analyzer (Felix Instruments, USA) through silicone septa stuck on the films. The avocados were cut open and their inner appearance observed, and flesh firmness tested on the 10th d for #1 and 20th d for #2. A simple experimental process is displayed in Fig. 1.

2.4.1. Gas composition in packaging headspace

According to the operating principles mentioned in section 2.3.6, not only ethylene content could be obtained, but also CO_2 and O_2 content were acquired. Finally, ethylene concentration was expressed as μmol/L, while O_2 and CO_2 concentrations were converted to mmol/L.

2.4.2. Avocado firmness

Avocado flesh firmness was measured using GY series fruit penetrometer (Shanghai Jingsheng Scientific Instruments Corporation, China) with a probe of 3.5 mm in diameter. Five testing points for each avocado were randomly measured after avocados were cut open and the firmness unit was converted to N.

2.4.3. Safety evaluation

After 20 d of preservation with LDPE-3%PKM, the packaged avocados were immersed in diluted nitric acid (HNO_3) solution for 24 h. The avocados without being packaged were as control. Then inductively coupled plasma-mass spectrometry (ICP-MS) was used to measure the concentrations of manganese (Mn), silicon (Si), and aluminum (Al) elements in the solution to figure out the migration of active agents (pumice and $KMnO_4$). The detailed processing method is introduced in our precious published article (Wang, C. and Ajji, A., 2022).

2.5. Statistical analysis

All experiments were carried out in three replicates and the statistical analysis of experimental data was performed using Minitab software (Minitab® 19 for windows, Minitab LLC, USA) according to one-way ANOVA with Tukey's test to ensure a significance level of $p \leq 0.05$. Graphs in this report were plotted in accordance with mean values and error bars were designed according to standard deviation.

3. Results and discussion

3.1. SEM and color analysis of films

Fig. 2(a–f) shows SEM cross-sectional images and surface color of LDPE-based films containing different content of active agents. Fig. 2 (a) is the SEM image of pure LDPE film whose cross-section is smooth. There is no conspicuous aggregation observed in the cross-section of films incorporating 1 wt% and 3 wt% of active agents, as presented in Fig. 2 (b) and (c). This is because PE-g-MA, as compatibilizer, was added to facilitate dispersion of active agents in LDPE matrix (Kahar et al., 2012; Mengual et al., 2017). To prove the effect of compatibilizer, the film containing 3 wt% of active agents without compatibilizer was also produced, and the particles aggregated apparently as depicted in Fig. S1. When 5 wt% of active agents was added, aggregation (i.e. the larger particles) appeared in Fig. 2 (d). Furthermore, Fig. 2 (e) shows that clearly visible aggregation occurred in LDPE-10%PKM, even though PE-g-MA was used, illustrating excess active agents were not able to achieve homogeneous dispersion. Therefore, choosing the appropriate content of active agents is of great importance during the process of melt blending because the degree of particle dispersion has a significant

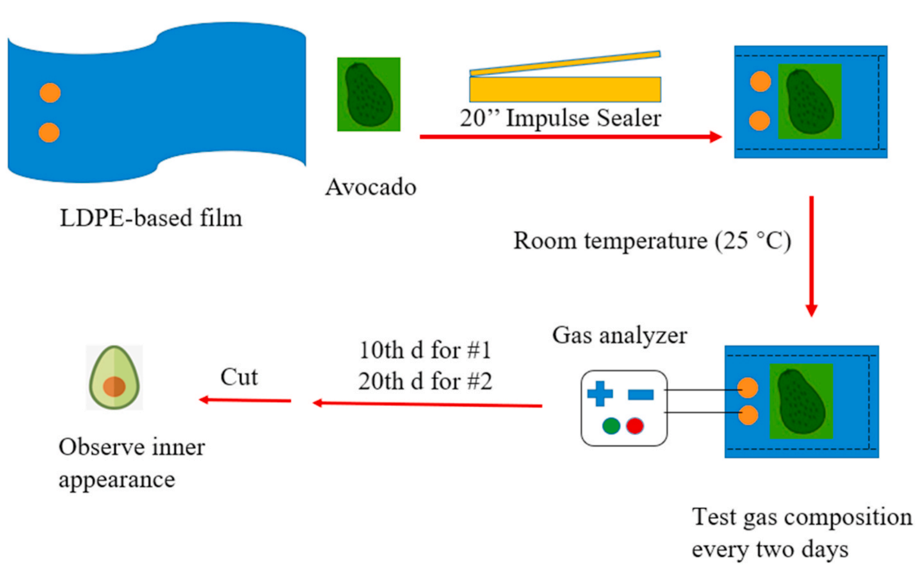

Fig. 1. The experimental process of packaging and observing avocados.

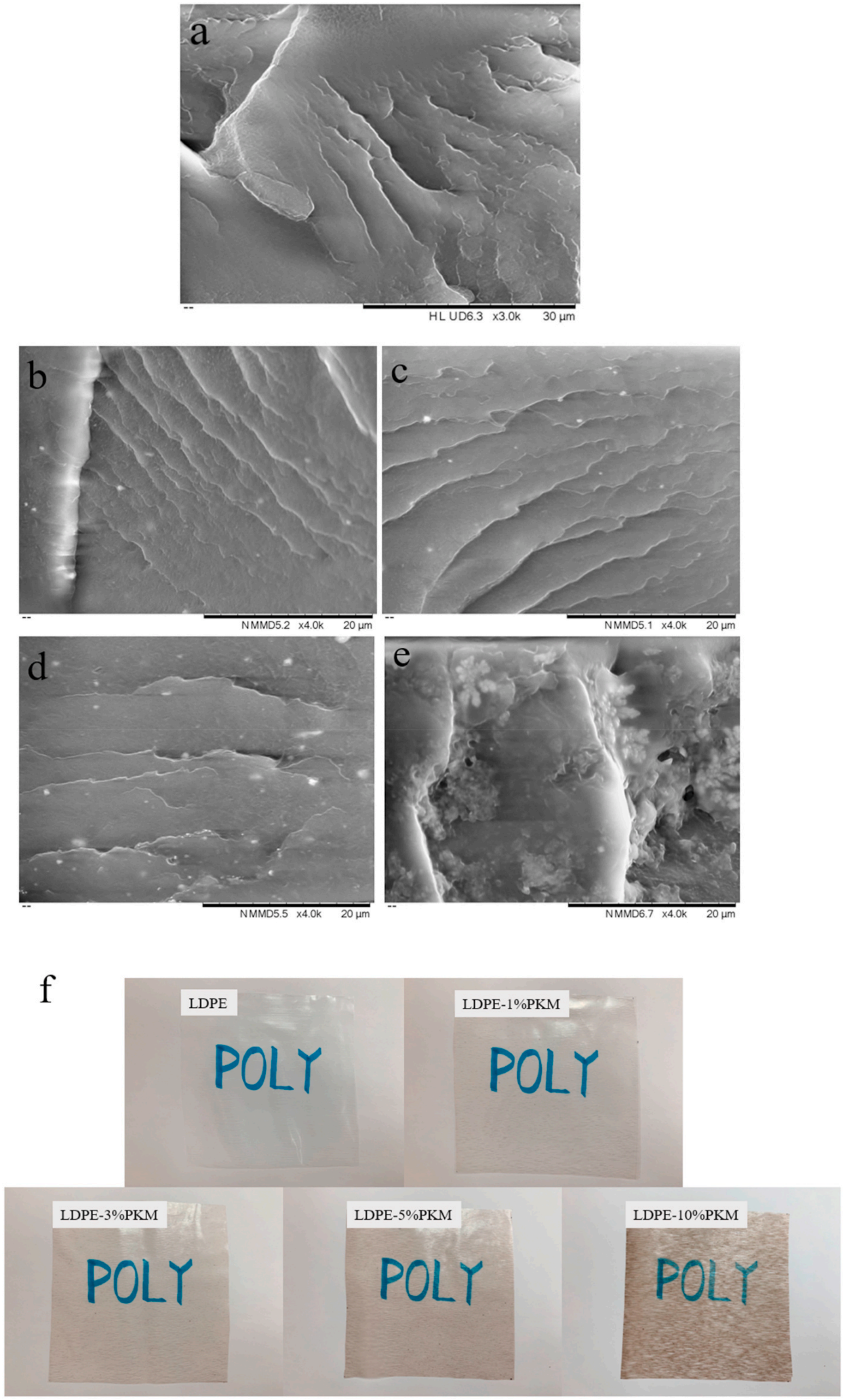

Fig. 2. SEM cross-sectional images of LDPE-based films: (a) LDPE, (b) LDPE-1%PKM, (c) LDPE-3%PKM, (d) LDPE-5%PKM, and (e) LDPE-10%PKM; (f) photographs of films.

impact on the performance of extruded films, including thermal, mechanical, and gas barrier properties (Ebrahimi et al., 2021; Tas et al., 2017; Zhu et al., 2008).

The surface color of packaging films is an important marketing parameter, and it is usually preferable if one can see the food status through packaging films. Fig. 2 (f) illustrates that pure LDPE film is transparent, and LDPE-based films gradually become rough and opaque with the content of active agents, which could be associated with their dispersion in the films as pictured in Fig. 2(a–e). Therefore, the color difference (ΔE*) between the films was more and more prominent as the loading of active agents increased (Kadam et al., 2021; Upadhyay et al., 2022). The ΔE* based on reference (color of pure LDPE film) was 2.80 for LDPE-1%PKM, 4.88 for LDPE-3%PKM, 10.89 for LDPE-5%PKM, and 21.31 for LDPE-10%PKM. The other color indices are summarized in the supplemental information.

3.2. FTIR

In order to figure out the influence of the addition of active agents and PE-g-MA on films, the FTIR spectra were collected in Fig. 3. Regarding FTIR spectra of LDPE-based films, five characteristic peaks were assigned to CH_2 asymmetric stretching (2850 and 2915 cm^{-1}), CH_3 symmetric deformation (1375 cm^{-1}), and bending deformation and rocking deformation (1465 and 720 cm^{-1}) (Gulmine et al., 2002). Because the main chain of PE-g-MA is comprised of polyethylene molecule, the spectrum of PE-g-MA also displayed the same bands as LDPE-based films, as can be observed in Fig. 3 and Fig. S2. In reality, PE-g-MA served as a bridge linking LDPE matrix and active agents, which increased the degree of dispersion of active agents, as explained in SEM section. The spectrum of PE-g-MA exhibited the small peaks at the range of 1710–1790 cm^{-1} attributed to the stretching vibration of C=O group (Oromiehie et al., 2013; Rodríguez et al., 2022), however, their disappearance on the spectra of ethylene scavenging films indicated the reaction between hydroxyl groups on the surface of pumice and maleic anhydride groups of PE-g-MA (Saini et al., 2017; Wang et al., 2011). As for active agents, a broad peak at 1030 cm^{-1} was caused by stretching vibrations of O-Si-O bonds coming from pumice (Bardakçı et al., 2012), and this peak slightly shifted to 1070 cm^{-1} for ethylene scavenging films, which could be also a hint of the bonding interaction between pumice and PE-g-MA (Bikiaris et al., 2005). In addition, the peak of $KMnO_4$ at 900 cm^{-1} (Becerra et al., 2011) was too weak to observe in the films, and its presence induced the small vibrational peaks around 2350 cm^{-1} that also appeared in the spectra of ethylene scavenging films.

3.3. DSC

Melting temperature (T_m) and melting enthalpy (ΔH_m) of films were determined through DSC thermograms. Crystallinity (X_c) was calculated according to the equation, $X_c = \frac{\Delta H_m}{\Delta H_f^0} \times 100\%$ (Joung et al., 2021; Li et al., 2019), where ΔH_f^0 is the heat of fusion taken as 293 J/g based on 100% crystalline LDPE (Molefi et al., 2010). The DCS graphs are displayed in Fig. S3 and the results in terms of T_m, ΔH_m, and X_c are summarized in Fig. 4. T_m was almost not influenced after the addition of active agents at a stable value of 108–109 °C. Compared with 61.4 J/g for pure LDPE, ΔH_m increased to 66.6 J/g for LDPE-1%PKM and 63.1 J/g for LDPE-3% PKM, but decreased to 60.1 J/g for LDPE-5%PKM and 50.5 J/g for LDPE-10%PKM. Correspondingly, X_c displayed the same trend, rising from 20.9% for pure LDPE to the maximal value at 22.7% for LDPE-1% PKM and then going down. At lower loadings (1 wt% and 3 wt%), the active agents acted as nucleating agents to induce crystallization of LDPE molecular chains due to uniform dispersion (Tas et al., 2017), however, the nucleating efficiency was diminished at higher loadings (5 wt% and 10 wt%) because of particle aggregation (Joung et al., 2021). A relationship can be built between crystallinity and gas permeability (Zabihzadeh Khajavi et al., 2020). The crystalline region of films is impermeable, so gas molecules need bypass the crystalline region to pass through films, which decreases the gas permeability of films. Therefore, a higher crystallinity normally stands for a lower gas permeability that will be introduced in section 3.5.

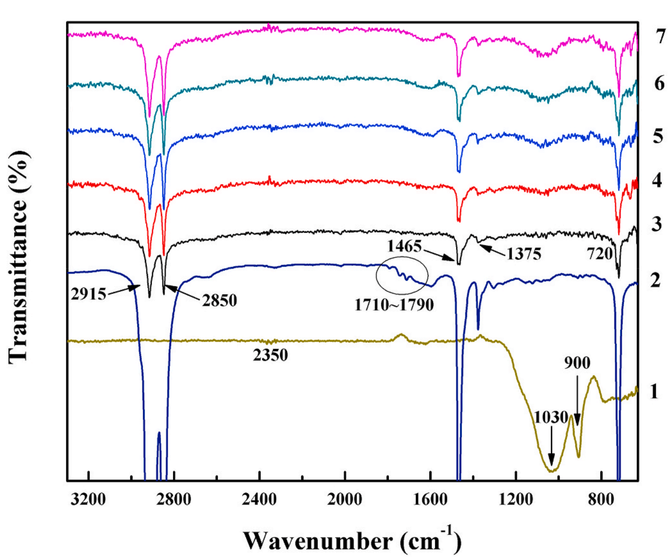

Fig. 3. FTIR spectra of (1) active agents (mixture of pumice and $KMnO_4$), (2) PE-g-MA, (3) pure LDPE, (4) LDPE-1%PKM, (5) LDPE-3%PKM, (6) LDPE-5% PKM, and (7) LDPE-10%PKM.

3.4. Mechanical properties

Mechanical properties of films were characterized, and the results are shown in Fig. 5. It is apparent that LDPE-3%PKM, compared with other films, exhibited optimum Young's modulus (307.39 MPa), tensile strength (9.51 MPa), and elongation at break (307.90%), followed by LDPE-1%PKM (286.26 MPa, 9.63 MPa, and 313.53% respectively), demonstrating that 1 wt% and 3 wt% of active agents improved mechanical performances of films. This is because low loadings of active agents dispersed uniformly in LDPE matrix as can be observed in SEM images (Fig. 2), and the degree of dispersion is involved with the mechanical properties. Relevant studies have reported that a small amount of clay additives with a good dispersion in polymer films resulted in an enhancement of mechanical properties (Abulyazied & Ene, 2021; Motawie et al., 2014; Pavlidou & Papaspyrides, 2008). However, mechanical performances were significantly diminished for LDPE-5%PKM (elongation at break decreased to 115.7%) and especially for LDPE-10% PKM (Young's modulus was reduced to 202.90 MPa, tensile strength to 4.20 MPa, and elongation at break to 15.33%). This can be explained that higher loadings of active agents led to the poor dispersion and particle aggregation in the LDPE matrix as discussed in SEM section.

3.5. Gas barrier properties

The gas barrier properties of films were evaluated according to their OTR and WVTR in Fig. 6. It is obvious that LDPE-3%PKM possessed the lowest OTR (1465.58 cc/[m^2·day]) and WVTR (24.31 g/[m^2·day]), meaning the film incorporated with 3 wt% active agents had better oxygen and water vapor barrier properties. Although OTR of LDPE-1% PKM was slightly higher by 4.12% than that of LDPE-3%PKM, both of their gas barrier performances were improved compared with pure LDPE film, and a similar result was reported that 1 wt% and 3 wt% of alkaline halloysite nanotubes greatly enhanced the gas barrier properties of LDPE film (Boonsiriwit et al., 2020). This result was expected because the tortuous paths for gas diffusion in the LDPE matrix were formed due to well-dispersed active agents at lower loadings (1 wt% and 3 wt%) (Azeredo, 2009; Muller et al., 2017). In addition, the presence of active agents at lower loadings increased the crystallinity, which also increased the gas barrier properties of films, as explained in section 3.3. On the contrary, higher loadings of active agents resulted in the formation of aggregation, especially evident at 10 wt%, leading to higher gas permeability and poor barrier performance (Joung et al., 2021; Tas et al., 2017).

3.6. Ethylene scavenging analysis

In general, pure LDPE film cannot remove ethylene, but the presence of active agents endows it with ethylene scavenging capacity. According to the curves in Fig. 7, it can be concluded that the ethylene scavenging capacity of LDPE-based films is correlated to the content and the

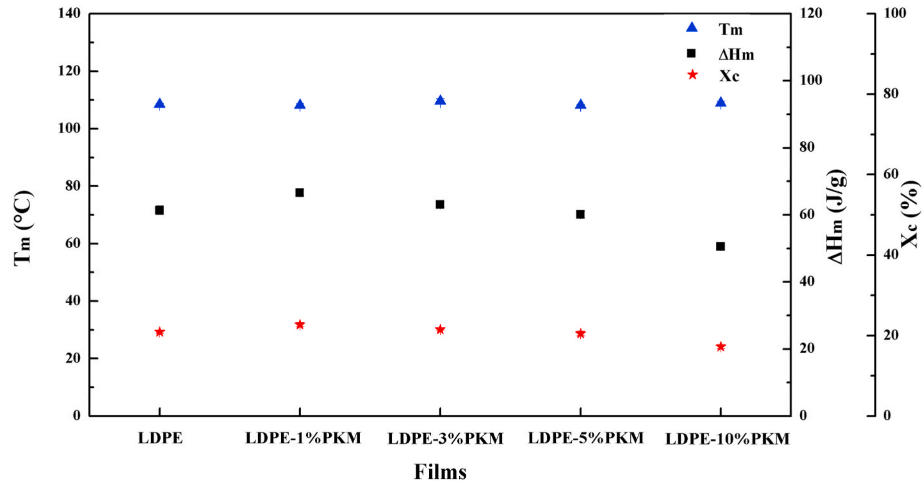

Fig. 4. Summary of DSC results (T_m, ΔH_m, X_c) for LDPE-based films.

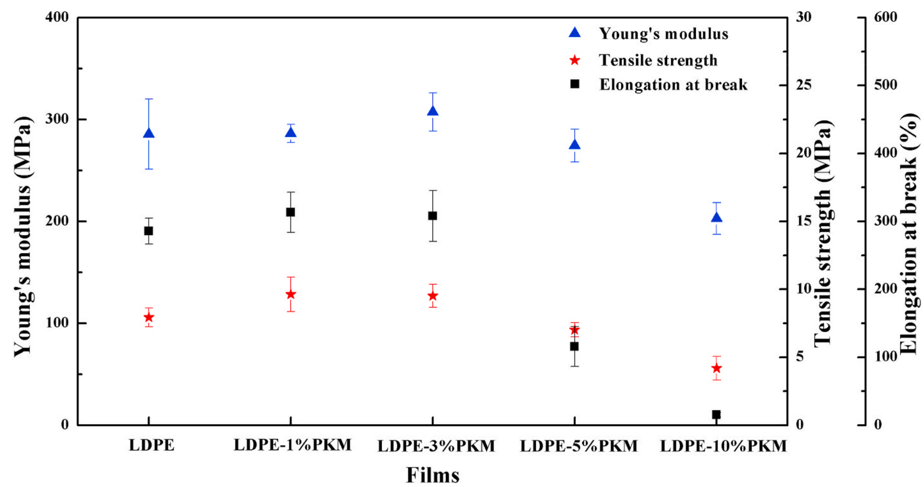

Fig. 5. Summary of mechanical properties for LDPE-based films.

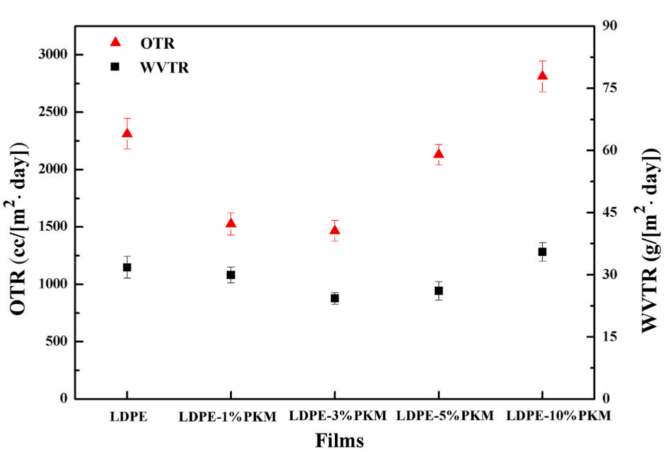

Fig. 6. Summary of OTR and WVTR for LDPE-based films.

dispersion of active agents (Ebrahimi et al., 2021; Joung et al., 2021). In the case of little difference of dispersion, the content of active agents determined the ethylene scavenging capacity of films, so LDPE-3%PKM could scavenge more ethylene than LDPE-1%PKM, and the same for LDPE-5%PKM and LDPE-10%PKM, as can be observed in Fig. 7. In addition, the ethylene scavenging capacity of LDPE-1%PKM and

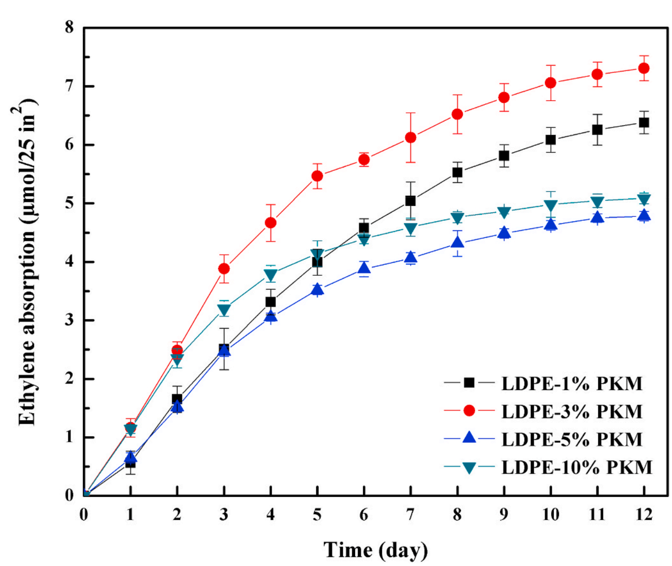

Fig. 7. Ethylene scavenging capacity of LDPE-based films.

LDPE-3%PKM are superior to that of LDPE-5%PKM and LDPE-10%PKM, which should be caused by the uniform dispersion of low loadings of active agents and the particle aggregation of high loadings. Taken together, 3 wt% of active agents are the most beneficial to the films with regards to scavenging ethylene. During a period of 12 d, LDPE-3%PKM had an ethylene scavenging capacity of 7.31 μmol/(25 in^2), followed by LDPE-1%PKM (6.38 μmol/(25 in^2)), LDPE-10%PKM (5.08 μmol/(25 in^2)) and LDPE-5%PKM (4.78 μmol/(25 in^2)). The result indicates that these films may extend the shelf life of fruit and vegetables by scavenging ethylene.

3.7. Preservation of avocados through ethylene scavenging films

3.7.1. Gas composition in packaging headspace

Gas composition is an important indicator to evaluate fruit status and three gases including ethylene, O_2, and CO_2 are involved during their ripening process. As a matter of fact, the three gases interact with each other, for example, the high ethylene concentration accelerates the respiration rate of fruit, leading to the low O_2 concentration and high CO_2 concentration, and vice versa. Herein, ethylene, O_2, and CO_2 concentrations within 20 d in the packaging headspace are displayed in Fig. 8 (a), (b), and (c) respectively. The avocados packaged with LDPE and LDPE-10%PKM were spoiled on the 10th d, so their data were not collected after 10 d.

It is well known that avocados are very sensitive to ethylene and controlling ethylene concentration as low as possible is beneficial to their preservation. Avocados belong to climacteric fruit meaning there is a climacteric stage for respiration rate and ethylene production rate (Paul et al., 2012; Zhang et al., 2017). For LDPE-1%PKM and LDPE-5% PKM packaging, ethylene concentration gradually increased and quickly peaked at 8.33 μmol/L and 5.53 μmol/L respectively on the 10th d, and then decreased until spoilage. Although a similar trend was found for LDPE-3%PKM packaging, the period of ethylene concentration reaching the peak was postponed to 12th d and the value was 3.44 μmol/L. During the first four days of storage, the ethylene concentration in the packaging headspace of LDPE and LDPE-10%PKM is approximately 1.0 μmol/L, higher by 150%–750% than that of the other three packaging, and later, the ethylene concentration in LDPE packaging increased to nearly 2.0 μmol/L, while it did not show significant fluctuation in LDPE-10%PKM packaging as can be observed in Fig. 8 (a). On the one hand, due to LDPE had no ethylene absorption capacity, the accumulated ethylene during the first few days resulted in the disordered respiration (Fig. 8 (b) and (c)) and the spoilage of avocado (Fig. 9 (a)). On the other, the poor gas barrier of LDPE-10%PKM caused the strong gas exchange between packaging headspace and surrounding atmosphere, leading to a high O_2 concentration (Fig. 8 (b)) and a low CO_2 concentration (Fig. 8 (c)) as well as the spoiled avocado (Fig. 9 (e)). By comparison, LDPE-3%PKM demonstrated a better performance in controlling ethylene concentration.

The changes of O_2 and CO_2 concentrations are reversed because CO_2 is produced when O_2 is consumed, as can be seen in Fig. 8 (b) and (c). As control, O_2 concentration in the packaging headspace of LDPE was kept at a low level around 2.63 mmol/L while CO_2 concentration was high, increasing from 4.90 mmol/L to 6.28 mmol/L. The poor gas barrier of LDPE-10%PKM induced a high O_2 concentration (nearly 7.07 mmol/L) and a low CO_2 concentration (below 1.99 mmol/L). In LDPE-1%PKM packaging, O_2 concentration significantly decreased to 2.83 mmol/L and CO_2 concentration rapidly increased to 6.67 mmol/L on the 10th d, whereas the corresponding value was 3.41 mmol/L and 4.86 mmol/L in LDPE-5%PKM packaging. In LDPE-3%PKM packaging, the minimal O_2 concentration and maximal CO_2 concentration were detected on the 12th d, at 4.36 mmol/L and 4.05 mmol/L respectively. Although the low O_2 concentration and high CO_2 concentration can inhibit the respiration rate of avocados (Maftoonazad & Ramaswamy, 2005; Yahia & Gonzalez-Aguilar, 1998), it is not always favorable to preserve avocados in such atmosphere. This is because anaerobic respiration occurs when

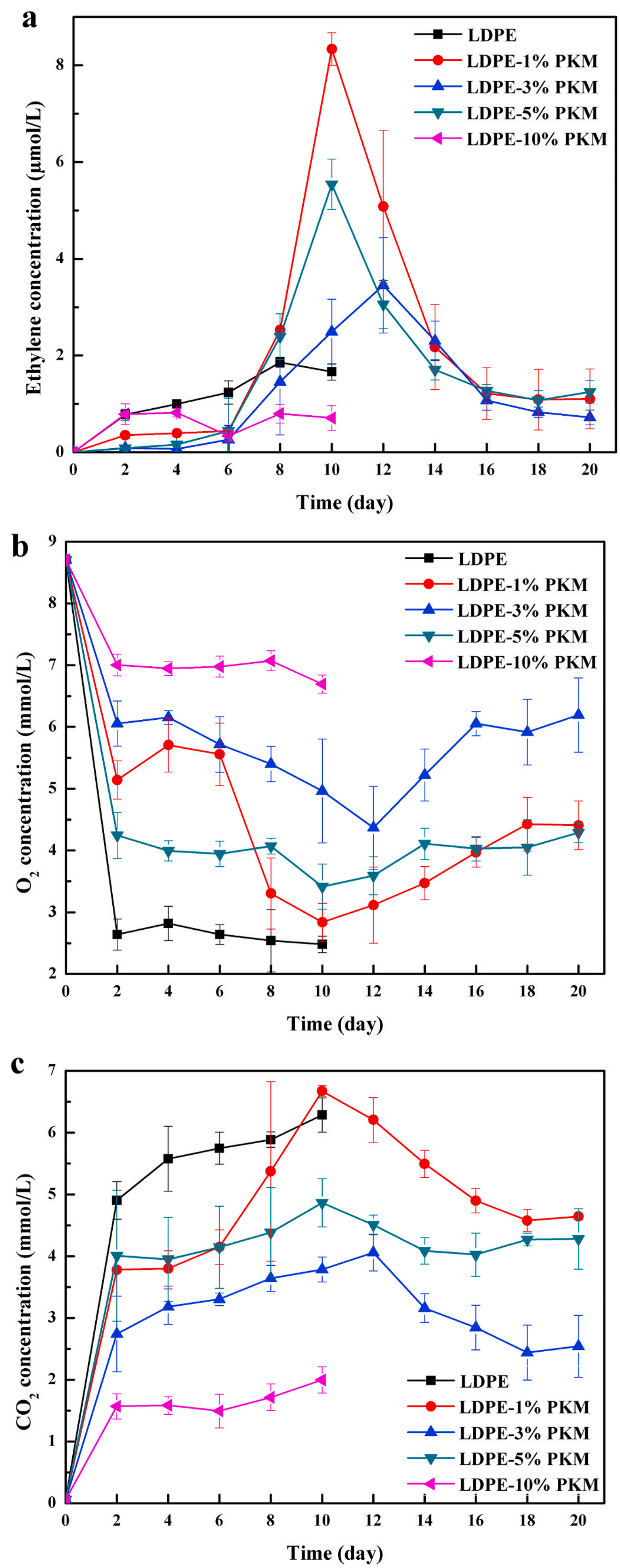

Fig. 8. Gas composition (a: ethylene, b: O_2, c: CO_2) in packaging headspace at 25 °C up to 20 d.

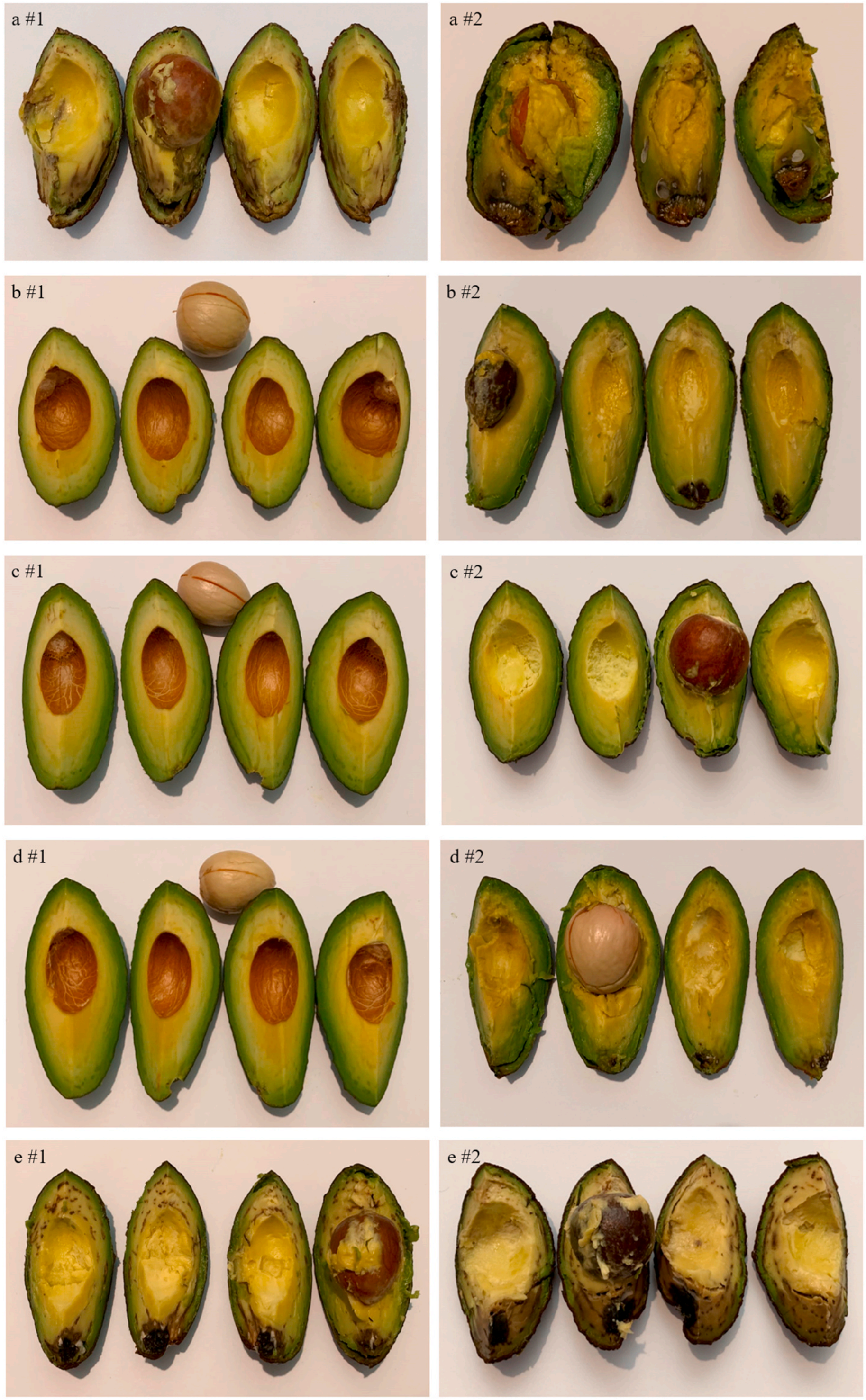

Fig. 9. Inner appearance of avocados packaged with (a) pure LDPE film, (b) LDPE-1%PKM, (c) LDPE-3%PKM, (d) LDPE-5%PKM, and (e) LDPE-10%PKM (#1: preservation for 10 d, #2: preservation for 20 d).

the level of O_2 is too low (<2%) (Berrios, 2002), and physiological injury is caused by too high CO_2 concentration (>15%) (Young et al., 1962). Meir et al. (1997) concluded that the optimal atmosphere conditions were 2–6% O_2 (corresponding to 0.89–2.68 mmol/L) and 3–10% CO_2 (corresponding to 1.35–4.50 mmol/L) at 5 °C and 7 °C. LDPE-3%PKM controlled CO_2 concentration to 1.35–4.50 mmol/L, which is the reason that it extended the shelf life of avocados to 20 d. Nonetheless, one limitation of this study is that the O_2 concentration was not adjusted to the optimal range.

3.7.2. *Shelf life and firmness of avocados*

The shelf life of avocados can be evaluated by inner appearance and flesh firmness. It is apparent that avocados packaged with LDPE and LDPE-10%PKM were spoiled during 10 d of storage according to the inner appearance (Fig. 9 (a #1) and (e #1)). In contrast, avocados preserved by LDPE-1%PKM, LDPE-3%PKM, and LDPE-5%PKM for 10 d were still in good condition (Fig. 9 (b #1) (c #1) and (d #1)). It can be attributed that pure LDPE film could not scavenge ethylene produced by avocado, while LDPE-10%PKM had poor gas barrier performance, meaning gas exchange between packaging headspace and atmosphere was uncontrolled and the respiration of avocado happened as under normal conditions. However, LDPE-1%PKM, LDPE-3%PKM, and LDPE-5%PKM not only scavenged ethylene but also had good gas barrier performance, which ensured that avocados were well preserved. Undoubtedly, LDPE and LDPE-10%PKM were not able to protect avocado for 20 d as can be observed in Fig. 9 (a #2) and (e #2). On the 20th d, black spots appeared on the bottom of flesh of avocados packaged with LDPE-1%PKM and LDPE-5%PKM as shown in Fig. 9 (b #2) and (d #2), nevertheless, inner appearance was free of defects regarding the avocado packaged with LDPE-3%PKM as can be seen in Fig. 9 (c #2). Overall, LDPE-3%PKM showed the best gas barrier properties among all films and its ethylene scavenging capacity was superior, so that it was the most appropriate to be applied in avocado preservation.

Besides, flesh firmness, summarized in Fig. 10, can partly reflect whether avocados are spoiled or not (Gamble et al., 2010; Kokawa et al., 2020), because the firmness gradually decreased from unripe period to decay. The flesh firmness was approximately 0.50 N for avocados packaged with LDPE and LDPE-10%PKM for 10 d. For those preserved by LDPE-1%PKM, LDPE-3%PKM, and LDPE-5%PKM, their flesh firmness was 5.56 N, 5.69 N, and 5.52 N respectively after 10 d of preservation, and then decreased by 63.6%, 61.4%, and 62.5% respectively 20 d later. In combination with inner appearance and flesh firmness, LDPE-10%PKM and LDPE were not appropriate to preserve avocados, while LDPE-1%PKM and LDPE-5%PKM could preserve avocados at least 10 d but less than 20 d. The optimum film was LDPE-3%PKM which extended the shelf life of avocados to 20 d or more.

3.7.3. Safety evaluation

In this study, the safety issue is one limitation because $KMnO_4$ is not friendly as mentioned in the Introduction section. When the ethylene scavenging films are applied to package avocados, it is very likely that active agents migrate to the peels. Although the peels of avocados will be peeled off before ingestion, the investigation on the migration of active agents is important to learn about safety issue and pave a pathway for future research. For the solution sample of control, Mn, Si, and Al concentrations were detected as 7.5 ± 2.2 μg/L, 104.5 ± 8.7 μg/L, and 58.1 ± 7.0 μg/L respectively. By comparison, the corresponding elemental concentrations of the solution samples soaking avocados packaged with LDPE-3%PKM were higher than that of control, at 43.1 ± 7.1 μg/L (Mn), 177.5 ± 14.8 μg/L (Si), and 71.9 ± 5.8 μg/L (Al), illustrating active agents ($KMnO_4$ and pumice) migrated from films to the peels. This demonstrated that the application of the ethylene scavenging film in packaging fruit and vegetables might cause safety hazards. Thus, this study proved the importance to focus on how to avoid such safety hazards in the active packaging realms. Based on this study, the relevant research actually has been carried out through the development of multilayer films, which was published in our previous report (Wang, C. and Ajji, A., 2022).

4. Conclusion

The ethylene scavenging films containing LDPE as matrix and the mixture of pumice and $KMnO_4$ as active agents were prepared to extend the shelf life of avocados. Compared with pure LDPE film, the addition of active agents caused a reduction in the transparency of films. SEM images showed that low loadings (1 wt% and 3 wt%) of active agents could disperse uniformly within LDPE matrix with the aid of PE-g-MA, but aggregation occurred at high loadings (5 wt% and 10 wt%). A uniform dispersion of active agents increased ΔH_m and crystallinity of films, of which the maximum was 66.6 J/g and 22.7% for LDPE-1%PKM followed by LDPE-3%PKM, while the aggregation induced an opposite effect. Overall, LDPE-3%PKM exhibited the optimal mechanical properties with Young's modulus of 307.39 MPa, tensile strength of 9.51 MPa, and elongation at break of 307.90%. Moreover, LDPE-3%PKM displayed better gas barrier performance (OTR of 1465.58 cc/[m^2·day] and WVTR of 24.31 g/[m^2·day]) and superior ethylene scavenging capacity of 7.31 μmol/(25 in^2) compared with other films. Consequently, avocados could be well preserved using LDPE-3%PKM, showing that it extended the shelf life of avocados to 20 d, controlled ethylene and CO_2 concentrations in the packaging headspace, and reduced the flesh firmness loss. Hence, this investigation provides a possibility of reducing food loss by means of ethylene scavenging films incorporating pumice and $KMnO_4$. There are still several limitations of this study, for example, how to avoid safety issues caused by the migration of active agents, and how to control O_2 concentration to the optimal range.

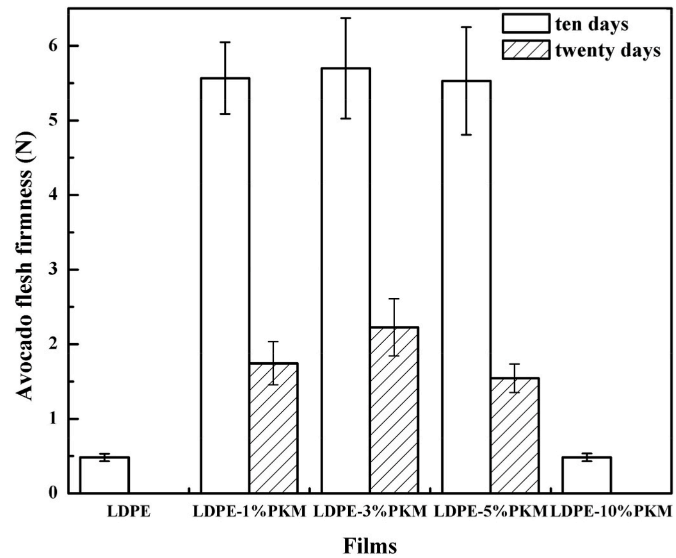

Fig. 10. Flesh firmness of avocados packaged with LDPE-based films for 10 d and 20 d.

CRediT authorship contribution statement

Chunyu Wang: Conceptualization, Data curation, Formal analysis, Investigation, Methodology, Writing – original draft. **Abdellah Ajji:** Supervision, Writing – review & editing.

Declaration of competing interest

The authors declare that they have no known competing financial interests or personal relationships that could have appeared to influence the work reported in this paper.

Data availability

Data will be made available on request.

Acknowledgements

The authors acknowledge financial support from 3SPack NSERC (Natural Sciences and Engineering Research Council of Canada). A scholarship is provided by the China Scholarship Council (CSC) to C. Wang.

Appendix A. Supplementary data

Supplementary data to this article can be found online at https://doi.org/10.1016/j.lwt.2022.114200.

References

Abulyazied, D. E., & Ene, A. (2021). An investigative study on the progress of nanoclay-reinforced polymers: Preparation, properties, and applications: A review. *Polymers (Basel), 13*(24). https://doi.org/10.3390/polym13244401

Álvarez-Hernández, M. H., Artés-Hernández, F., Ávalos-Belmontes, F., Castillo-Campohermoso, M. A., Contreras-Esquivel, J. C., Ventura-Sobrevilla, J. M., & Martínez-Hernández, G. B. (2018). Current scenario of adsorbent materials used in ethylene scavenging systems to extend fruit and vegetable postharvest life. *Food and Bioprocess Technology, 11*(3), 511–525. https://doi.org/10.1007/s11947-018-2076-7

Álvarez-Hernández, M. H., Martínez-Hernández, G. B., Avalos-Belmontes, F., Castillo-Campohermoso, M. A., Contreras-Esquivel, J. C., & Artés-Hernández, F. (2019a). Potassium permanganate-based ethylene scavengers for fresh horticultural produce as an active packaging. *Food Engineering Reviews, 11*(3), 159–183. https://doi.org/10.1007/s12393-019-09193-0

Álvarez-Hernández, M. H., Martínez-Hernández, G. B., Avalos-Belmontes, F., Miranda-Molina, F. D., & Artés-Hernández, F. (2020). Postharvest quality retention of apricots by using a novel sepiolite–loaded potassium permanganate ethylene scavenger. *Postharvest Biology and Technology, 160*. https://doi.org/10.1016/j.postharvbio.2019.111061

Álvarez-Hernández, M. H., Martínez-Hernández, G. B., Avalos-Belmontes, F., Rodríguez-Hernández, A. M., Castillo-Campohermoso, M. A., & Artés-Hernández, F. (2019b). An innovative ethylene scrubber made of potassium permanganate loaded on a protonated montmorillonite: A case study on blueberries. *Food and Bioprocess Technology, 12*(3), 524–538. https://doi.org/10.1007/s11947-018-2224-0

Azeredo, H. M. C.d. (2009). Nanocomposites for food packaging applications. *Food Research International, 42*(9), 1240–1253. https://doi.org/10.1016/j.foodres.2009.03.019

Bardakçı, B., Kaya, N., & Kalaycı, T. (2012). Anisidine adsorption on Co-supported pumice. *Environmental Earth Sciences, 70*(2), 849–856. https://doi.org/10.1007/s12665-012-2173-2

Becerra, M. E., Arias, N. P., Giraldo, O. H., López Suárez, F. E., Illán Gómez, M. J., & Bueno López, A. (2011). Soot combustion manganese catalysts prepared by thermal decomposition of KMnO4. *Applied Catalysis B: Environmental, 102*(1–2), 260–266. https://doi.org/10.1016/j.apcatb.2010.12.006

Berrios, J.d. J. (2002). Development of a dynamically modified atmosphere storage system applied to avocados. *Food Science and Technology International, 8*(3), 155–162. https://doi.org/10.1177/1082013202008003163

Bikiaris, D. N., Vassiliou, A., Pavlidou, E., & Karayannidis, G. P. (2005). Compatibilisation effect of PP-g-MA copolymer on iPP/SiO2 nanocomposites prepared by melt mixing. *European Polymer Journal, 41*(9), 1965–1978. https://doi.org/10.1016/j.eurpolymj.2005.03.008

Blanke, M. M. (2014). Reducing ethylene levels along the food supply chain: A key to reducing food waste? *Journal of the Science of Food and Agriculture, 94*(12), 2357–2361. https://doi.org/10.1002/jsfa.6660

Boonsiriwit, A., Xiao, Y., Joung, J., Kim, M., Singh, S., & Lee, Y. S. (2020). Alkaline halloysite nanotubes/low density polyethylene nanocomposite films with increased ethylene absorption capacity: Applications in cherry tomato packaging. *Food Packaging and Shelf Life, 25*. https://doi.org/10.1016/j.fpsl.2020.100533

Cevik, S. E., Yesil, O., Ozturk, T. C., & Guneysel, O. (2012). Potassium permanganate ingestion as a suicide attempt. *Clinical Practice, 2*(2), e32. https://doi.org/10.4081/cp.2012.e32

Dash, S., Patel, S., & Mishra, B. K. (2009). Oxidation by permanganate: Synthetic and mechanistic aspects. *Tetrahedron, 65*(4), 707–739. https://doi.org/10.1016/j.tet.2008.10.038

Ebrahimi, A., Zabihzadeh Khajavi, M., Mortazavian, A. M., Asilian-Mahabadi, H., Rafiee, S., Farhoodi, M., & Ahmadi, S. (2021). Preparation of novel nano–based films impregnated by potassium permanganate as ethylene scavengers: An optimization study. *Polymer Testing, 93*. https://doi.org/10.1016/j.polymertesting.2020.106934

Gaikwad, K. K., Singh, S., & Negi, Y. S. (2019). Ethylene scavengers for active packaging of fresh food produce. *Environmental Chemistry Letters, 18*(2), 269–284. https://doi.org/10.1007/s10311-019-00938-1

Gamble, J., Harker, F. R., Jaeger, S. R., White, A., Bava, C., Beresford, M., Stubbings, B., Wohlers, M., Hofman, P. J., Marques, R., & Woolf, A. (2010). The impact of dry matter, ripeness and internal defects on consumer perceptions of avocado quality and intentions to purchase. *Postharvest Biology and Technology, 57*(1), 35–43. https://doi.org/10.1016/j.postharvbio.2010.01.001

Gulmine, J. V., Janissek, P. R., Heise, H. M., & Akcelrud, L. (2002). Polyethylene characterization by FTIR. *Polymer Testing, 21*(5), 557–563. https://doi.org/10.1016/s0142-9418(01)00124-6

Heibati, B., Rodriguez-Couto, S., Amrane, A., Rafatullah, M., Hawari, A., & Al-Ghouti, M. A. (2014). Uptake of Reactive Black 5 by pumice and walnut activated carbon: Chemistry and adsorption mechanisms. *Journal of Industrial and Engineering Chemistry, 20*(5), 2939–2947. https://doi.org/10.1016/j.jiec.2013.10.063

Ismail, A. I., El-Shafey, O. I., Amr, M. H., & El-Maghraby, M. S. (2014). Pumice characteristics and their utilization on the synthesis of mesoporous minerals and on the removal of heavy metals. *International Scholarly Research Notices.* , Article 259379. https://doi.org/10.1155/2014/259379, 2014.

Joung, J., Boonsiriwit, A., Kim, M., & Lee, Y. S. (2021). Application of ethylene scavenging nanocomposite film prepared by loading potassium permanganate-impregnated halloysite nanotubes into low-density polyethylene as active packaging material for fresh produce. *Lebensmittel-Wissenschaft & Technologie, 145*. https://doi.org/10.1016/j.lwt.2021.111309

Kadam, A. A., Singh, S., & Gaikwad, K. K. (2021). Chitosan based antioxidant films incorporated with pine needles (Cedrus deodara) extract for active food packaging applications. *Food Control, 124*. https://doi.org/10.1016/j.foodcont.2021.107877

Kahar, A. W. M., Ismail, H., & Othman, N. (2012). Effects of polyethylene-grafted maleic anhydride as a compatibilizer on the morphology and tensile properties of (thermoplastic tapioca starch)/(high-density polyethylene)/(natural rubber) blends. *Journal of Vinyl and Additive Technology, 18*(1), 65–70. https://doi.org/10.1002/vnl.20289

Keller, N., Ducamp, M. N., Robert, D., & Keller, V. (2013). Ethylene removal and fresh product storage: A challenge at the frontiers of chemistry. Toward an approach by photocatalytic oxidation. *Chemistry Review, 113*(7), 5029–5070. https://doi.org/10.1021/cr900398v

Khosravi, R., Hashemi, S. A., Sabet, S. A., & Rezadoust, A. M. (2013). Thermal, dynamic mechanical, and barrier studies of potassium permanganate-LDPE nanocomposites. *Polymer-Plastics Technology and Engineering, 52*(2), 126–132. https://doi.org/10.1080/03602559.2012.719056

Kokawa, M., Hashimoto, A., Li, X., Tsuta, M., & Kitamura, Y. (2020). Estimation of 'hass' avocado (Persea americana mill.) ripeness by fluorescence fingerprint measurement. *Food Analytical Methods, 13*(4), 892–901. https://doi.org/10.1007/s12161-020-01705-7

Kordjazi, Z., & Ajji, A. (2021). Development of TiO2 catalyzed HTPB based oxygen scavenging films for food packaging applications. *Food Control, 121*. https://doi.org/10.1016/j.foodcont.2020.107639

Li, D., Zhou, L., Wang, X., He, L., & Yang, X. (2019). Effect of crystallinity of polyethylene with different densities on breakdown strength and conductance property. *Materials (Basel), 12*(11). https://doi.org/10.3390/ma12111746

Maftoonazad, N., & Ramaswamy, H. S. (2005). Postharvest shelf-life extension of avocados using methyl cellulose-based coating. *LWT - Food Science and Technology, 38*(6), 617–624. https://doi.org/10.1016/j.lwt.2004.08.007

Meir, S., Naiman, D., Akerman, M., Hyman, J. Y., Zauberman, G., & Fuchs, Y. (1997). Prolonged storage of Hass' avocado fruit using modified atmosphere packaging. *Postharvest Biology and Technology, 12*(1), 51–60. https://doi.org/10.1016/s0925-5214(97)00038-0

Mengual, A., Juárez, D., Balart, R., & Ferrándiz, S. (2017). PE-g-MA, PP-g-MA and SEBS-g-MA compatibilizers used in material blends. *Procedia Manufacturing, 13*, 321–326. https://doi.org/10.1016/j.promfg.2017.09.083

Molefi, J. A., Luyt, A. S., & Krupa, I. (2010). Comparison of LDPE, LLDPE and HDPE as matrices for phase change materials based on a soft Fischer–Tropsch paraffin wax. *Thermochimica Acta, 500*(1–2), 88–92. https://doi.org/10.1016/j.tca.2010.01.002

Monprasit, P., Ritvirulh, C., Sooknoi, T., Rukchonlatee, S., Fuongfuchat, A., & Sirikittikul, D. (2011). Selective ethylene-permeable zeolite composite double-layered film for novel modified atmosphere packaging. *Polymer Engineering & Science, 51*(7), 1264–1272. https://doi.org/10.1002/pen.21924

Motawie, A. M., Madani, M., Esmail, E. A., Dacrorry, A. Z., Othman, H. M., Badr, M. M., & Abulyazied, D. E. (2014). Electrophysical characteristics of polyurethane/organo-bentonite nanocomposites. *Egyptian Journal of Petroleum, 23*(4), 379–387. https://doi.org/10.1016/j.ejpe.2014.09.005

Muller, K., Bugnicourt, E., Latorre, M., Jorda, M., Echegoyen Sanz, Y., Lagaron, J. M., Miesbauer, O., Bianchin, A., Hankin, S., Bolz, U., Perez, G., Jesdinszki, M., Lindner, M., Scheuerer, Z., Castello, S., & Schmid, M. (2017). Review on the processing and properties of polymer nanocomposites and nanocoatings and their applications in the packaging, automotive and solar energy fields. *Nanomaterials (Basel), 7*(4). https://doi.org/10.3390/nano7040074

NCBI. (2022). *National center for biotechnology information. PubChem compound summary for CID 516875, potassium permanganate.* https://pubchem.ncbi.nlm.nih.gov/compound/Potassium-permanganate. (Accessed 23 July 2022).

Oromiehie, A. R., lari, T. T., & Rabiee, A. (2013). Physical and thermal mechanical properties of corn starch/LDPE composites. *Journal of Applied Polymer Science, 127*(2), 1128–1134. https://doi.org/10.1002/app.37877

Pathak, N., Caleb, O. J., Geyer, M., Herppich, W. B., Rauh, C., & Mahajan, P. V. (2017). Photocatalytic and photochemical oxidation of ethylene: Potential for storage of fresh produce—a review. *Food and Bioprocess Technology, 10*(6), 982–1001. https://doi.org/10.1007/s11947-017-1889-0

Paul, V., Pandey, R., & Srivastava, G. C. (2012). The fading distinctions between classical patterns of ripening in climacteric and non-climacteric fruit and the ubiquity of ethylene-An overview. *Journal of Food Science & Technology, 49*(1), 1–21. https://doi.org/10.1007/s13197-011-0293-4

Pavlidou, S., & Papaspyrides, C. D. (2008). A review on polymer–layered silicate nanocomposites. *Progress in Polymer Science, 33*(12), 1119–1198. https://doi.org/10.1016/j.progpolymsci.2008.07.008

Rad, T. S., Khataee, A., Kayan, B., Kalderis, D., & Akay, S. (2018). Synthesis of pumice-TiO2 nanoflakes for sonocatalytic degradation of famotidine. *Journal of Cleaner Production, 202*, 853–862. https://doi.org/10.1016/j.jclepro.2018.08.165

Reesha, K. V., Panda, S. K., Bindu, J., & Varghese, T. O. (2015). Development and characterization of an LDPE/chitosan composite antimicrobial film for chilled fish storage. *International Journal of Biological Macromolecules, 79*, 934–942. https://doi.org/10.1016/j.ijbiomac.2015.06.016

Rodríguez, L. J., Álvarez-Láinez, M. L., & Orrego, C. E. (2022). Optimization of processing conditions and mechanical properties of banana fiber-reinforced polylactic acid/high-density polyethylene biocomposites. *Journal of Applied Polymer Science, 139*(3), Article 51501. https://doi.org/10.1002/app.51501

Saini, A., Yadav, C., Bera, M., Gupta, P., & Maji, P. K. (2017). Maleic anhydride grafted linear low-density polyethylene/waste paper powder composites with superior mechanical behavior. *Journal of Applied Polymer Science, 134*(31), Article 45167. https://doi.org/10.1002/app.45167

Singh, N., & Lee, D. G. (2001). Permanganate: A green and versatile industrial oxidant. *Organic Process Research & Development, 5*(6), 599–603. https://doi.org/10.1021/op010015x

Sultana, A., Siddiqui, M. W., & Gaikwad, K. K. (2022). Synthesis of zeolitic imidazolate framework-8 composite as ethylene scavenger for fruits and vegetables preservation and packaging. *Biomass Conversion and Biorefinery*. https://doi.org/10.1007/s13399-022-03066-z

Tas, C. E., Hendessi, S., Baysal, M., Unal, S., Cebeci, F. C., Menceloglu, Y. Z., & Unal, H. (2017). Halloysite nanotubes/polyethylene nanocomposites for active food packaging materials with ethylene scavenging and gas barrier properties. *Food and Bioprocess Technology, 10*(4), 789–798. https://doi.org/10.1007/s11947-017-1860-0

Upadhyay, A., Kumar, P., Kardam, S. K., & Gaikwad, K. K. (2022). Ethylene scavenging film based on corn starch-gum acacia impregnated with sepiolite clay and its effect on quality of fresh broccoli florets. *Food Bioscience, 46*. https://doi.org/10.1016/j.fbio.2022.101556

Wang, C., & Ajji, A. (2022a). Development and application of low-density polyethylene-based multilayer film incorporating potassium permanganate and pumice for avocado preservation. *Food Chemistry, 401*, Article 134162. https://doi.org/10.1016/j.foodchem.2022.134162

Wang, C., & Ajji, A. (2022b). Development of a novel ethylene scavenger made up of pumice and potassium permanganate and its effect on preservation quality of avocados. *Journal of Food Engineering, 330*. https://doi.org/10.1016/j.jfoodeng.2022.111101

Wang, N., Gao, N., Jiang, S., Fang, Q., & Chen, E. (2011). Effect of different structure MCM-41 fillers with PP-g-MA on mechanical and crystallization performances of polypropylene. *Composites Part B: Engineering, 42*(6), 1571–1577. https://doi.org/10.1016/j.compositesb.2011.04.012

Wei, H., Seidi, F., Zhang, T., Jin, Y., & Xiao, H. (2021). Ethylene scavengers for the preservation of fruits and vegetables: A review. *Food Chemistry, 337*, Article 127750. https://doi.org/10.1016/j.foodchem.2020.127750

Widayanti, S. M., Syamsu, K., Warsiki, E., & Yuliani, S. (2016). *Effect of natural Bayah zeolite particle size reduction to physico-chemical properties and absortion against potassium permanganate (KMnO4)*. AIP Conference Proceedings. AIP Publishing LLC, Article 030029.

Wills, R. B. H., & Warton, M. A. (2004). Efficacy of potassium permanganate impregnated into alumina beads to reduce atmospheric ethylene. *Journal of the American Society for Horticultural Science, 129*(3), 433–438. https://doi.org/10.21273/jashs.129.3.0433

Wyrwa, J., & Barska, A. (2017). Innovations in the food packaging market: Active packaging. *European Food Research and Technology, 243*(10), 1681–1692. https://doi.org/10.1007/s00217-017-2878-2

Yahia, E. M., & Gonzalez-Aguilar, G. (1998). Use of passive and semi-active atmospheres to prolong the postharvest life of avocado fruit. *LWT - Food Science and Technology, 31*(7–8), 602–606. https://doi.org/10.1006/fstl.1998.0383

Young, R. E., Romani, R. J., & Biale, J. B. (1962). Carbon dioxide effects on fruit respiration . II. Response of avocados, bananas, & lemons. *Plant Physiol, 37*(3), 416–422. https://doi.org/10.1104/pp.37.3.416

Zabihzadeh Khajavi, M., Ebrahimi, A., Yousefi, M., Ahmadi, S., Farhoodi, M., Mirza Alizadeh, A., & Taslikh, M. (2020). Strategies for producing improved oxygen barrier materials appropriate for the food packaging sector. *Food Engineering Reviews, 12*(3), 346–363. https://doi.org/10.1007/s12393-020-09235-y

Zhang, J., Cheng, D., Wang, B., Khan, I., & Ni, Y. (2017). Ethylene control technologies in extending postharvest shelf life of climacteric fruit. *Journal of Agricultural and Food Chemistry, 65*(34), 7308–7319. https://doi.org/10.1021/acs.jafc.7b02616

Zhu, A., Cai, A., Zhang, J., Jia, H., & Wang, J. (2008). PMMA-grafted-silica/PVC nanocomposites: Mechanical performance and barrier properties. *Journal of Applied Polymer Science, 108*(4), 2189–2196. https://doi.org/10.1002/app.27863